RSC Advances

ROYAL SOCIETY OF CHEMISTRY

www.rsc.org/advances

Tartaric acid modified *Pleurotus ostreatus* for enhanced removal of Cr(VI) ions from aqueous solution: characteristics and mechanisms

Weihua Xu[a,b,*], Shufan Wang[a,b], Yunguo Liu[a,b], Guangming Zeng[a,b], Bohong Zheng[c], XiaoFei Tan[a,b], Tinjting Li[a,b], Hui Wang[a,b], Fangying Guo[a,b], Mingming Zhang[a,b],

[a] College of Environmental Science and Engineering, Hunan University, Changsha 410082, PR China

[b] Key Laboratory of Environmental Biology and Pollution Control (Hunan University), Ministry of Education, Changsha 410082, PR China

[c] School of Architecture and Art, Central South University, Changsha 410082, PR China

[*] Corresponding author. Tel: +86 15116358984; fax: +86 731 88822829.

E-mail address: hnuesexwh@gmail.com (W.H. Xu)

Abstract

The *Pleurotus ostreatus* was modified by tartaric acid and used as biosorbent for the removal of Cr(VI) from aqueous solution. The removal efficiency of Cr(VI) by the modified *P. ostreatus* was 2 to 2.5 times higher than by pristine. FTIR and XPS analysis indicated that carboxyl and amino groups were the major functional groups for Cr(VI) sorption. Batch sorption experiments were carried out to investigate the characteristic and adsorption behavior of MPOD. Experimental data fitted pseudo-second order equation and Freundlich isotherm. The optimum biosorption was observed at pH 2.0 with the biosorption capacity of 99.66 mg g^{-1}. Thermodynamic analysis showed that the adsorption process was spontaneous and endothermic. The present results confirmed that electrostatic attraction and complexation were involved in Cr(VI) removal. Modified *P. ostreatus* has the characteristics of simplicity and obvious effects for the removal of Cr(VI) ions from aqueous solution.

Keywords

Modified *P. ostreatus*; Cr(VI) ions; Biosorption; tartaric acid

1. Introduction

Environmental contamination caused by heavy metals has become an issue of growing concern due to their health risks on humans and animals. Chromium is a priority pollutant because of its high toxicity and frequent occurrence in polluted sites.[1] Chromium exists in two main oxidation states in the environment: Cr(VI) and Cr(III). Compared to Cr(III), Cr(VI) is more toxic due to its carcinogenic and mutagenic effect for living organisms.[2] Therefore chromium is widely recognized to exert toxic effects in its hexavalent form.[3] Several wastewaters from manufacturing process, such as dyes and pigments production, metal cleaning, plating and electroplating, may contain undesirable amounts of Cr(VI) ions.[4] Unregulated disposal of the chromium containing effluent in both developing and developed countries has led to the contamination of surface and ground waters.[5] So that, the

removal of Cr(VI) from wastewater is significant in the protection of environment and human health.

Various methods for the removal of heavy metal ions from wastewater have already existed, including chemical precipitation, electrolytic reduction, ion exchange, membrane filtration, activated carbon adsorption, etc. However these technologies may have disadvantages like less effective, incomplete removal, high reagent cost, energy needs and secondary pollution[6]. Thus, it is imperative to find out a new cost-effective treatment method, to remove heavy metals from effluents.[7] It is well known that cellulosic waste materials can be obtained and employed as cheap adsorbents, such as modified corn stalks, orange waste, sugar beet tailing, modified ramie fiber and so on.[8-11]

Macro-fungi have shown good potential as materials for the remediation of wastewater containing toxic metal ions. As a fungus, *Pleurotus ostreatus* is a useful source of mycelia biomass for biosorption of metal ions because of its easy cultivation, high yield and non-hazardous nature.[7] It is one of the most common edible mushrooms in China and grows prolifically in many parts of the world, which is macro in size, tough in texture and has other physical characteristics conducive for development as a biosorbent.[12] It is a material with great source of cellulose, hemicelluloses, and lignin, and its performance to remove heavy metal ions can be affected upon chemical treatment. Some pre-treatments have been done to change surface properties and increase the biosorption capacity of the fungal biomass, for example, heat, acid and/or alkali treatment.[13] Numerous chemicals also have been used for modification which include mineral, organic acids, oxidizing agent, organic compounds, etc.[14] Some authors have described the functional carboxylic and the hydroxyl groups of the celluloses as the active binding sites for metals, as these groups can attract and sequester the heavy metal ions.[8,15]

In this study, *P. ostreatus* was modified by tartaric acid to enhance the biosorption capacity for Cr(VI) removal . Fourier transform infrared spectroscopy

(FTIR) and X-ray photoelectron spectroscopy (XPS) were employed to qualify the major functional groups responsible for the removal of Cr(VI) anions. In addition, a series of batch sorption tests were performed to investigate the parameters, which could evaluate the adsorption capacity and characteristics of modified *P. ostreatus* powder (MPOD) as a sorbent for the removal of Cr(VI) from aqueous solution. The sorption process was investigated by isothermic, kinetic and themodynamic analysis to study the biosorption characteristic of Cr(VI) on MPOD.

2. Materials and methods

2.1. Main instruments and materials

All chemicals (analytical grade) used in this study were purchased from local chemical suppliers and used without any treatment. Tartaric acid (white crystal power) was obtained from Shanghai Shanpu Chemical Co., Ltd.. Cr(VI) stock solution of 1000 mg L^{-1} was prepared by dissolving 2.8290 g of K_2CrO_4 in 1000 mL ultrapure water and all the working solutions were subsequently obtained by diluting the stock solution. The concentration of Cr(VI) was determined by measuring the absorbance of the purple complex of Cr(VI) with 1,5–diphenylcarbohydrazide at 540 nm using a UV spectrophotometer (Pgeneral T6, China).

2.2. Sample preparation

Fungal tailing of *P. ostreatus* (POD) was collected from vegetable market. POD was washed with distilled water and dried at 80 °C for 24 h before use. The biomass were ground in a mortar to powder and sieved through a 100 mesh sieve. After that, the biomass were mixed up with tartaric acid powder, and the mass ratio of *P. ostreatus* powder to tartaric acid was 1:2. Then distilled water was gradually added into the mixture. The sample was shaken at 130 r min^{-1} and 50 °C for 24 h. After the

heating response, the mixture was filtered and washed with ultra-pure water to remove the unreacted tartaric acid. The obtained new materials (MPOD) was dried in an oven at 60 ºC for 4 h and finally stored at room temperature.

2.3. Characterization of POD and MPOD

The surface morphologies of the prepared samples were characterized by a field emission scanning electron microscopy (SEM) (JSM–7001F, Japan).

Fourier transform infrared spectrum (Nicolet 5700 Spectrometer) measurements were carried out to identify the functional groups involved in the metal removal. The FTIR spectra of the adsorbent were recorded in the range of 4000–400 cm^{-1}.The elements of POD and MPOD were determined by an ESCALAB 250Xi X–ray Photoelectron Spectrometer (XPS) (Thermo Fisher, USA). Binding energies (BEs) of the spectra was performed with the C1s neutral carbon peak at 284.6eV with accuracy of $\pm$0.05 eV.

2.4. Batch adsorption studies

All the adsorption experiments were carried out as follows: 0.1 g of adsorbent was added to 100 mL flasks containing 50 mL of Cr(VI) ions solution. The initial pH was adjusted to the needed values by HCl or NaOH solutions (0.1–1.0 mol L^{-1}) . Flasks were shaken at 130 r min^{-1} at the needed temperature. Removal efficiency (E_R) was expressed as Eq. (1):

$$E_R = \frac{C_0 - C}{C_0} \times 100\,\% \quad (1)$$

where C_0 and C (mg L^{-1}) are the initial and residual concentrations of metal ion, respectively .

To study the effect of initial concentrations on Cr(VI) ion adsorption, MPOD were added to several flasks with different concentration of Cr(VI) (20, 50, 80, 100

and 200 mg L^{-1}). After adjusted the solution pH to 4.0, the flasks were shaken at 50 °C for 24 h.

The study of the pH dependency of Cr(VI) ion adsorption on MPOD was carried out as follows: MPOD was added to five flasks containing 50 mg L^{-1} Cr(VI) ions solution, the pH value was adjusted to 2.0, 3.0, 4.0, 5.0, 6.0, 7.0, 8.0, 9.0 and 10.0, respectively. Flasks were shaken at 50 °C for 24 h.

Kinetic biosorption experiments were carried out at pH 2.0, 50 °C with initial Cr(VI) concentration of 100 mg L^{-1}. The residual concentration of Cr(VI) was determined after designated time periods (5, 10, 30, 60, 120, 180, 360, 720, 1080, 1440 and 2880 min).

For isotherm and thermodynamic analysis, the experiments were studied at different initial Cr(VI) concentration (20, 50, 80, 100, 200, 250, 400 and 500 mg L^{-1}) at 30, 40, and 50 °C respectively.

All experimental data were the average of triplicate determinations and the relative errors of the data were about 5%.

3. Results and discussion

3.1. Characterization of POD,MPOD

3.1.1. SEM

The surface morphologies of POD, MPOD and MPOD + Cr (after adsorption of Cr on MPOD) were observed using SEM. POD shows uneven and irregular surface (Fig. 1.a), while MPOD (Fig. 1.b) was relatively smoother than POD. The probable reason was that carboxylic acid treatment could solubilize lignin and hemicelluloses during the esterification reaction. After biosorption of Cr(VI), the surface of the biosorbent became smooth and well-knit dramatically (Fig. 1.c), which was possibly due to the adsorption of Cr(VI) ions on the surface of MPOD biomass after 24 hours

of reaction.

3.1.2. FTIR and XPS analysis

To better understand how chemical modification affected the functional groups on *P. ostreatus*, Fourier transform infrared (FTIR) spectroscopy and X-ray photoeletron spectroscopy (XPS) were conducted on POD, MPOD, and MPOD + Cr. The FTIR spectra are presented in Fig. 2. As shown in Fig. 2, the spectra displayed a number of adsorption peaks indicating the complex nature of the biomass. The broad adsorption peak around 3400 cm^{-1} is assigned to –OH stretching vibrations and the peak at 2922 cm^{-1} attributed to –CH stretching.[16,17] The broad adsorption peak became weak after modification because the surface hydroxyls of the POD biomass were reacted with carboxyl group during the esterification reaction. The new peaks detected on the MPOD biomass at 1650–1780 cm^{-1} represent a chelate form of the carbonyl on the carboxyl group. This peak was described as the region of uncoordinated COO^- groups and ionized coordinated COO^- groups, respectively.[16,18] The new peaks confirmed that carboxyl was introduced onto POD after modified by tartaric acid. The new bands appeared at 1540 and 1223cm^{-1}, corresponding to N–H and C–N bond stretching, respectively, which confirmed the presence of amide functional group.[7,19] Therefore, it could be concluded that $–NH_2$, –OH and –COOH groups were involved in binding the metals.

XPS analysis was performed on POD and MPOD to gain further information on its chemical composition. As shown in Fig. 3(a), the C1s XPS spectrum of POD can be curve-fitted into four peak components at approximately 284.4 eV (C–C), 284.8 eV (non-oxygenated ring C), 286.2 eV (C–O) and 287.7 eV (C–O–C).[20,21] As seen from Fig. 3(b), the C1s XPS spectrum of MPOD clearly indicates a fairly high degree of oxidation with five components that correspond to C–C (284.2 eV), C–C/C–H (284.6 eV), C–N (285.9 eV), N–C=O (287.8 eV) and O–C=O (288.3 eV).[15,22] On the basis of the XPS results, the main difference between POD and MPOD is the new peak of

ester bond (288.3 eV). That may be attributed to the fact that the *P. ostreatus* is a material with great source of cellulose, hemicelluloses, and lignin. Hydroxyl group of the cellulose could react with carboxyl anhydride which dehydrated from tartaric acid and formed ester bond. The reaction process was as follows:

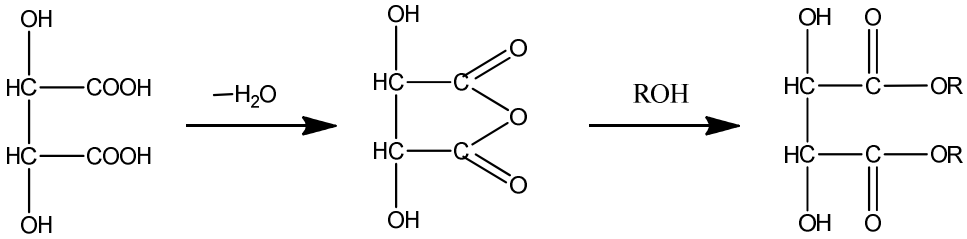

A B (2)

where A is tartaric acid, R is the pristine *P. ostreatus*, and B is tartaric acid modified *P. ostreatus*.

Thus, it can be concluded that carboxyl has been introduced successfully to the *P. ostreatus* surface. And the introduction of carboxyl can enhance the ability of the modified material to remove Cr(VI) ions by chelation reaction.[23]

The peak around 400 eV is attributed to N1s, N1s XPS spectrum in Fig. 3 (c) and (d) indicates a considerable degree of surface modification with the amino group. The shoulder appeared in the N1s region at 401.4eV most likely results from a small amount of the terminal amines that have acquired a proton.[24] Following the reaction with tartaric acid, a large N1s peak at 399.5 eV appeared. The results suggested that the *P. ostreatus* was functionalized well with free NH_2 groups, which was in agreement with FTIR results.

3.2. Adsorption studies

3.2.1. Influence of initial concentration of Cr(VI)

The effects of initial Cr(VI) concentration on Cr(VI) removal are shown in Fig. 4. It indicated that the adsorption capacity of the MPOD was obviously improved after modification. The Cr(VI) removal efficiency of both MPOD and POD was decreased with the increasing initial Cr(VI) concentration. The removal efficiency of Cr(VI)

decreased from 78.7% to 32.3% (MPOD) and 34.5% to 18.1% (POD) when the initial Cr(VI) concentration increased from 20 to 200 mg^{-1}, respectively. This was due to the fact that the total available surface binding sites were finite for a fixed adsorbent dosage, thus a decrease in percentage removal corresponding to an increase of initial Cr(VI) concentration occurred.[8]

3.2.2. Influence of solution pH

It is well known that the pH of the aqueous solution is an important parameter of biosorption of metal ions. As seen from Fig. 5, the maximum biosorption was observed at pH 2.0. The biosorption efficiency of Cr(VI) ions by MPOD decreased when the solution pH increased. At the pH increased from 2.0 to 6.0, the adsorption efficiency for Cr(VI) decreased dramatically from 98.4% to 24.3%, and the removal capacity gradually reached an asymptotic value at pH 6.0 to 10.0. This is because the solution pH affects the major form of the chromium ion, protonation level, and the charge (ionization state) of surface functional groups. At lower pH (1–4), the major form of Cr(VI) is $HCrO_4^-$ while the amine groups were positively charged (Eq.(3)).[25]

$$M–NH_2 + H^+ \rightarrow M–NH_3^+ \quad (3)$$

At lower pH values, the overall surface charge on the biomass became positive or less negative, which will promote a stronger coulombic attraction towards negatively charged Cr(VI) complex ions in the solution.[26] Besides, there is a high concentration of OH^- at higher pH, which could compete with Cr(VI) ions for the binding sites and result in a decreased sorption of Cr(VI).[21]

3.2.3. Kinetic model

Fig. 6(a) represents the effect of contact time on Cr(VI) sorption on MPOD. As shown in Fig. 6(a), Cr(VI) sorption process included two stages. The first 6 h involved rapid metal sorption process which may due to the abundant availability of active binding sites on the adsorbent. Over 65% of the total Cr(VI) removal occurred

in this stage. Then the subsequent slow adsorption of Cr(VI) continued for a longer period of time until sorption equilibrium was attained. The sorption became less efficient in this stage.

Pseudo-first-order equation and pseudo second-order equation were employed to model the sorption data over the entire time range. The pseudo-first-order equation is generally expressed as follows:

$$\log(q_e - q_t) = \log q_e - \frac{k_1}{2.303} t \quad (4)$$

where k_1 is the rate constant of pseudo-first-order biosorption (min L^{-1}), q_e and q_t denote the amounts of biosorption at equilibrium and at time t (mg g^{-1}), respectively.

The pseudo-second-order kinetic rate equation was derived on the basis of the biosorption capacity of the solid phase. The pseudo-second-order kinetic rate equation is expressed as:

$$\frac{t}{q_t} = \frac{1}{k_2 q_e^2} + \frac{t}{q_e} \quad (5)$$

where k_2 is the rate constant of pseudo-second-order adsorption (g mg^{-1} min^{-1}).

In this paper the pseudo-first-order kinetic model was not shown because the experimental data were not in good agreement. Fig. 6(b) showed a plot of t/q_t and t of biosorption of Cr (VI) for the pseudo-second-order equation, from which q_e and k_2 can be determined from the slope and intercept of the plot, respectively. The kinetic parameters for Cr(VI) adsorption were given in Table 1. The correlation coefficients for the pseudo-first-order and pseudo-second-order equation were 0.98 and 0.99 respectively. But the calculated q_e values of the pseudo-second-order agreed better than the pseudo-first-order equation. This strongly suggested that the biosorption of Cr(VI) on MPOD was most appropriately represented by a pseudo-second-order rate process. The good fit of the data to this model implied that the biosorption of Cr(VI) by MPOD was chemisorption, involving ion exchange and chelating reaction potentially.

3.2.4. Isotherm studies

In this study, two widespread-used isotherm models (Eq. (6) and Eq. (8)) were applied to describe the equilibrium characteristics of the adsorption.

The Langmuir model assumes that a monomolecular layer is formed when adsorption takes place without any interaction between the adsorbed molecules.[27] The Langmuir model was represented as:

$$q_e = \frac{q_{\max} K_L C_e}{1 + K_L C_e} \quad (6)$$

$$R_L = \frac{1}{1 + K_L C_0} \quad (7)$$

where $q$max (mg g^{-1}) is the maximum adsorption capacity, C_0 (mg L^{-1}) and C_e (mg L^{-1}) are the initial and the equilibrium solute concentration of Cr(VI), respectively. K_L (L mg^{-1}) is the Langmuir affinity constant related to adsorption energy, R_L is the equilibrium parameter which can be applied to predict if the adsorption system is favorable ($0<R_L<1$) or unfavorable ($R_L>1$).

The Freundlich isotherm model is an empirical equation based on heterogeneous surfaces suggesting that binding sites are not equivalent and/or independent.[28] The Freundlich model is represented as:

$$q_e = K_F C_e^{1/n} \quad (8)$$

where q_e (mg g^{-1}) is the adsorption capacity at equilibrium concentration, C_e (mg L^{-1}) is the equilibrium solute concentration, K_F and n are the Freundlich constants related to adsorption capacity and adsorption intensity, respectively.

The parameters of Langmuir and Freundlich isotherm models are shown in Fig.7 and Table 2. It was obvious that temperature of 50 °C showed the highest capacity for Cr(VI) adsorption by MPOD. The maximum adsorption capacity was close to 100 mg g^{-1}. The maximum biosorption capacity was 102.21 mg g^{-1} when the temperature increased to 60 °C. This result indicated that the optimum temperature of Cr(VI)

sorption on MPOD was 50 °C. The Freundlich isotherm model was appropriate for the results with the higher correlation coefficient R^2 than that of Langmuir. This indicates that the heterogeneity sorption of Cr(VI) ions to the binding sites, and that may be attributed to the active groups on the MPOD surface, such as –OH, –COO− groups and so on.[29] The *n* values in this study were calculated in the range from 2.43 to 4.15, indicating that the adsorption between metal ions and adsorbent was favorable (1<n<10). The larger value of *n* implied stronger interaction between adsorbent and heavy metal.[11,28]

3.2.5. Thermodynamic analysis

The results on the effect of temperature indicated that the maximum adsorption of Cr(VI) ions was obtained at 50 °C. The adsorption capacity of Cr(VI) increased from 69.48 mg g^{-1} to 99.66 mg g^{-1} as temperature increased from 30 °C to 50 °C, suggesting that the sorption process probably underwent chemical rather than physical interaction.[30] The rise in sorption capacity is due to the increase in collision frequency between biosorbent and adsorbate, which resulted in the enhanced adsorption of Cr(VI) ions from aqueous solution.[31] The results revealed that Cr(VI) adsorption is an endothermic process, as verified by the following calculation of thermodynamic parameters.

Thermodynamic parameters such as Gibbs free energy change (ΔG^0), enthalpy change (ΔH^0) and entropy change (ΔS^0) for the adsorption of Cr(VI) have been determined by using the following equations:

$$\Delta G^0 = -RTK^0 \quad (9)$$

$$\ln K^0 = -\frac{\Delta H^0}{RT} + \frac{\Delta S^0}{R} \quad (10)$$

where R (8.314 J mol^{-1} K^{-1}) is the universal gas constant, T (K) is the absolute temperature , K^0 can be calculated by plotting ln K_d (K_d=q_e/C_e) versus C_e and extrapolating C_e to zero. The values of ΔH^0 and ΔS^0 can be obtained from the slope

and intercept of a plot of ln K^0 against $1/T$ from the Fig. 8. Thermodynamic analysis was investigated at three different temperatures (30, 40, and 50 °C). The calculated results were given in Table 3. It was obvious that the ΔG^0 values became more negative as the temperature increased, which suggested that the adsorption is spontaneity and more favorable at high temperature. The standard enthalpy and entropy changes of adsorption were determined from Fig. 8 to be 52.63 kJ mol^{-1} and 175.32 J $mol^{-1}K^{-1}$, respectively. The value of ΔH^0 was positive, which proved that the adsorption was an endothermic process. The positive value of ΔS^0 suggested the increase of randomness at the solution interface during the biosorption of metal ions.[32]

4. Conclusions

In the present study, the advantages of using *P. ostreatus* as the source of a new adsorbent lie primarily in its high abundance and low cost. Tartaric acid modified method has the characteristics of simplicity and obvious effects. The aim of this work was to determine the biosorption characteristics and mechanisms of modified *P. ostreatus* for removal of Cr(VI) ions. FTIR and XPS analysis confirmed that carboxyl and amino groups were introduced onto POD after modification with tartaric acid. These function groups were essential for capturing Cr(VI) from aqueous solutions.

The MPOD could be efficiently used for biosorption of Cr(VI) ions, the removal efficiency of Cr(VI) by MPOD was 2 to 2.5 times higher than by POD. The biosorption capacity decreased as initial Cr(VI) concentration increased. The biosorption of Cr(VI) ions by MPOD decreased with the increase of pH from 2.0–6.0. Pseudo-second-order and Freundlich model described the adsorption processes well, indicating that the adsorption processes is mainly controlled by chemical sorption. The maximum adsorption capacity obtained from Freundlich model was 99.66 mg g^{-1}. Thermodynamic parameters were calculated. The thermodynamic study revealed the spontaneity, endothermic and irreversibility natures of Cr(VI) biosorption. Results obtained from this study showed that modified *P. ostreatus* is an effective and

environmental friendly absorbent for the removal of Cr(VI) ions from aqueous solution.

Acknowledgements

This work was supported by the National Natural Science Foundation of China (51108167 and 51478470) and the Fundamental Research Funds for the Central Universities, Hunan University.

328 **References**

329 1 Y.S. Shen, S.L. Wang, Y.M. Tzou, Y.Y. Yan, W.H. Kuan, Bioresour. *Technol.*,
330 2012, 104, 165–172.

331 2 Y. Zhang, H.L. Ma, J. Peng, M. Zhai, Z.Z. Yu, *J. Mater. Chem.*, 2012, 22,
332 5914–5916.

333 3 D.W. O'Connell, C. Birkinshaw, T.F. O'Dwyer, *Bioresour. Technol.*, 2008, 99,
334 6709–6724.

335 4 X.S. Wang, Y.P. Tang, S.R. Tao, *Chem. Eng. J.*, 2009, 148, 217–225.

336 5 N. Ertugay, Y.K. Bayhan, *J. Hazard. Mater.*, 2008, 154, 432–439.

337 6 P. Xu, G.-M. Zeng, D.-L. Huang, C.L. Feng, S. Hu, M.-H. Zhao, C. Lai, Z. Wei, C.
338 Huang, G.-X. Xie, Z.-F. Liu, *Sci. Total. Environ.*, 2012, 424, 1–10.

339 7 A. Javaid, R. Bajwa, U. Shafique, J. Anwar, *Biomass Bioenergy*, 2011, 35,
340 1675–1682.

341 8 S. Chen, Q. Yue, B. Gao, Q. Li, X. Xu, *Chem. Eng. J.*, 2011, 168, 909–917.

342 9 A.B. Perez-Marin, V.M. Zapata, J.F. Ortuno, M. Aguilar, J. Saez, M. Llorens, *J.*
343 *Hazard. Mater.*, 2007, 139, 122–131.

344 10 X. Dong, L.Q. Ma, Y. Li, *J. Hazard. Mater.*, 2011, 190, 909–915.

345 11 Z. Sun, Y. Liu, Y. Huang, X. Tan, G. Zeng, X. Hu, Z. Yang, *J. Colloid. Interf. Sci.*,
346 2014, 434C, 152–158.

347 12 R. Vimala, N. Das, *J. Hazard. Mater.*, 2009, 168, 376–382.

348 13 G. Bayramoglu, G. Celik, E. Yalcin, M. Yilmaz, M.Y. Arica, *J. Hazard. Mater.*,
349 2005, 119, 219–229.
350 14 W.S. Wan Ngah, M.A.K.M. Hanafiah, *Bioresour. Technol.*, 2008, 99, 3935-3948.
351 15 L.Q. Xu, D. Wan, H.F. Gong, K.G. Neoh, E.T. Kang, G.D. Fu, *Langmuir*, 2010,
352 26, 15376–15382.
353 16 X.F. Tan, Y.G. Liu, G.M. Zeng, X. Wang, X.J. Hu, Y.L. Gu, Z.Z. Yang,
354 *Chemosphere*, 2015, doi:10.1016/j.chemosphere.2014.12.058.
355 17 R. Vimala, N. Das, *J. Enviro. Sci.*, 2011, 23, 288–293.
356 18 J.L.Gardea-Torresdey., K.D., K.J.Tiemann., J.G.Parsons., J.Ramos.,
357 N.E.Pingitore., G.Gamez, *Microchem. J.*, 2002, 71, 157–166.
358 19 T. Ramanathan, F.T. Fisher, R.S. Ruoff, L.C. Brinson, *Chem. Mater.*, 2005, 17
359 1290–1295.
360 20 S. Stankovich, D.A. Dikin, R.D. Piner, K.A. Kohlhaas, A. Kleinhammes, Y. Jia, Y.
361 Wu, S.T. Nguyen, R.S. Ruoff, *Carbon*, 2007, 4, 1558–1565.
362 21 H. Wang, Y.G. Liu, G.M. Zeng, X.J. Hu, X. Hu, T.T. Li, H.Y. Li, Y.Q. Wang, L.H.
363 Jiang, *Carbohyd. Poly.*, 2014, 11, 166–173.
364 22 V. Datsyuk, M. Kalyva, K. Papagelis, J. Parthenios, D. Tasis, A. Siokou, I.
365 Kallitsis, C. Galiotis, *Carbon*, 2008, 46, 833–840.
366 23 F. Gode, E. D. Atalay, E. Pehlivan, *J. Hazard. Mater.*, 2008, 152, 1201–1207.
367 24 R. Stine, J.W. Ciszek, D.E. Barlow, W.K. Lee, J.T. Robinson, P.E. Sheehan,
368 *Langmuir*, 2012, 28, 7957–7961.

25 H.-L. Ma, Y. Zhang, Q.-H. Hu, D. Yan, Z.-Z. Yu, M. Zhai, *J. Mater. Chem.*, 2012, 22, 5914-5916.

26 J.-L. Gong, B. Wang, G.-M. Zeng, C.-P. Yang, C.-G. Niu, Q.-Y. Niu, W.-J. Zhou, Y. Liang, *J. Hazard. Mater.*, 2009, 164, 1517–1522.

27 X.J. Hu, J.S. Wang, Y.G. Liu, X. Li, G.M. Zeng, Z.L. Bao, X.X. Zeng, A.W. Chen, F. Long, *J. Hazard. Mater.*, 2011, 185, 306–314.

28 M. Lu, Y.-G. Liu, H. Xin-jiang., Y. Ben, X.-X. Z, T.T. Li, H. Wang, *J. Cent. South Univ.*, 2013, 20, 2478–2488.

29 H. Wang, Y.G. Liu, X.J. Hu, T.T. Li, *J. Cent. South Univ.*, 2014, 21, 2810–2818.

30 G.X. Yang, *H. Jiang, Water Res.*, 2014, 48, 396–405.

31 Y. Khambhaty, K. Mody, S. Basha, B. Jha, *Chem. Eng. J.*, 2009, 145, 489–495.

32 T. Fan, Y. Liu, B. Feng, G. Zeng, C. Yang, M. Zhou, H. Zhou, Z. Tan, X. Wang, *J. Hazard. Mater.*, 2008, 160, 655–661.

Figure captions:

Fig. 1. SEM images of POD (a), MPOD (b) and after adsorption of Cr(VI) on MPOD (c).

Fig. 2. FTIR spectra of POD, MPOD and adsorption of Cr(VI) on MPOD.

Fig. 3. -XPS spectra of POD and MPOD. a) C1s XPS spectrum of POD. b) C1s XPS spectrum of MPOD. c) N1s XPS spectrum of POD. d) N1s XPS spectrum of MPOD.

Fig. 4. Influence of initial Cr(VI) concentration on Cr(VI) adsorption by POD and MPOD.

Fig. 5. Influence of solution pH on Cr(VI) adsorption by MPOD.

Fig. 6. -Kinetics of Cr(VI) adsorption onto MPOD at 50 °C (initial Cr(VI) concentration 100 mg L^{-1}; pH: 2.0). a) Cr(VI) sorption kinetics data; b) pseudo second-order model for Cr(VI) sorption.

Fig. 7. Langmuir and Freundlich isotherm for biosotption of Cr(VI) on MPOD (Cr(VI) solution volume: 50 mL; adsorbent dose: 0.1 g; contact time: 24 h; pH: 2.0).

Fig. 8. Plot of $\ln K^0$ versus $1/T$ for estimation of thermodynamic parameters for the biosorption of Cr(VI) on MPOD. (Volume, 50 mL; biosorbent dose: 2.0 g; initial Cr(VI) concentration: 20, 50, 80, 100, 200, 250, 400, 500 mg L^{-1}; pH: 2.0; contact time: 24 h.)

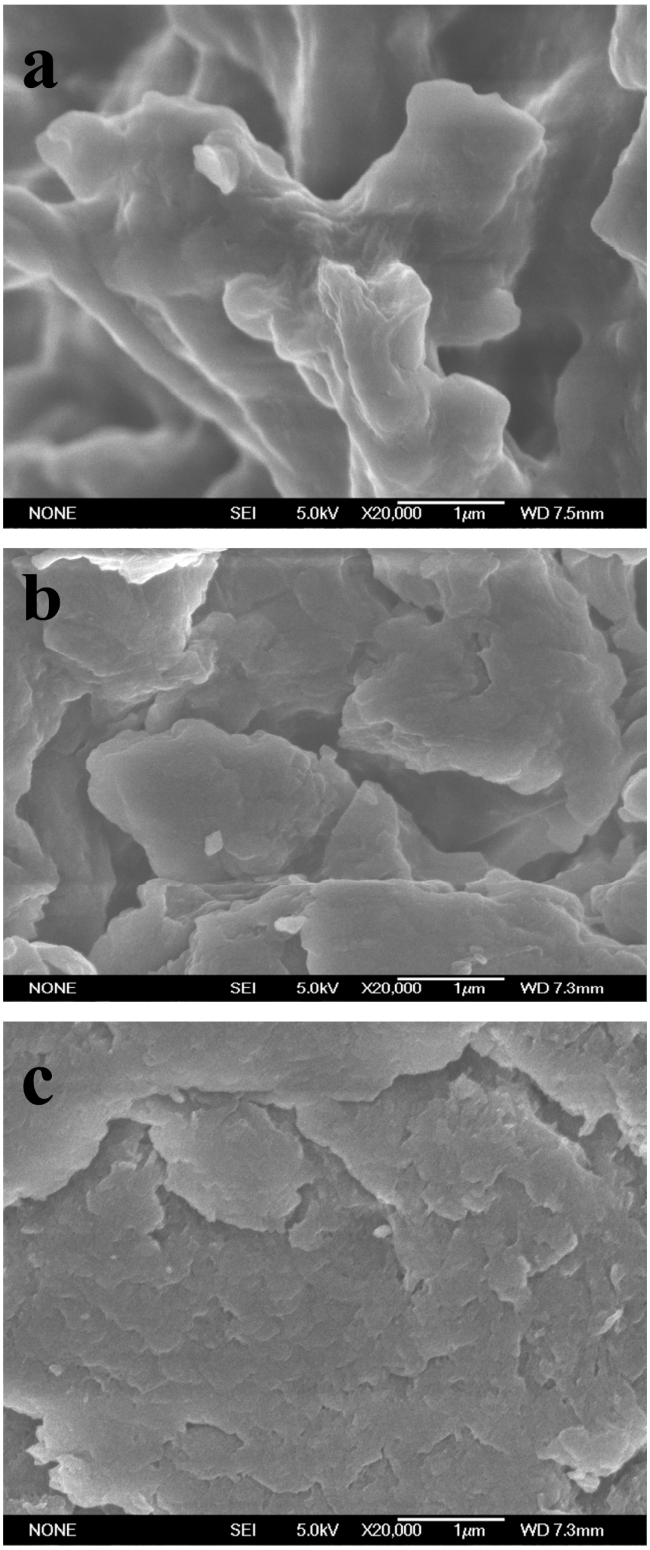

Fig. 1. SEM images of POD (a), MPOD (b) and after adsorption of Cr(VI) on MPOD (c).

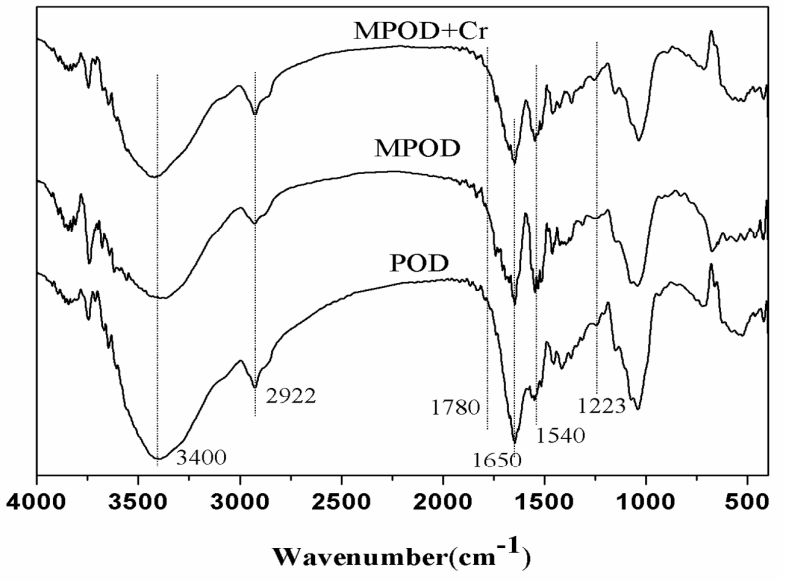

Fig. 2. FTIR spectra of POD, MPOD and adsorption of Cr(VI) on MPOD.

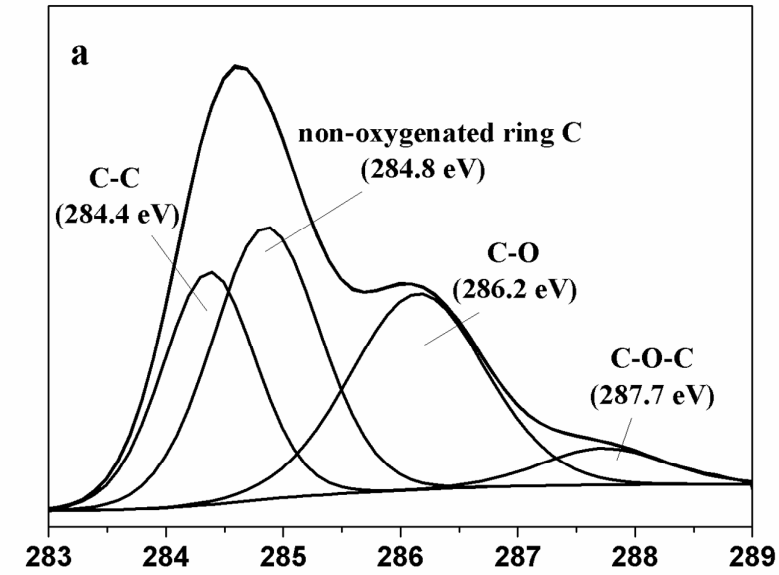

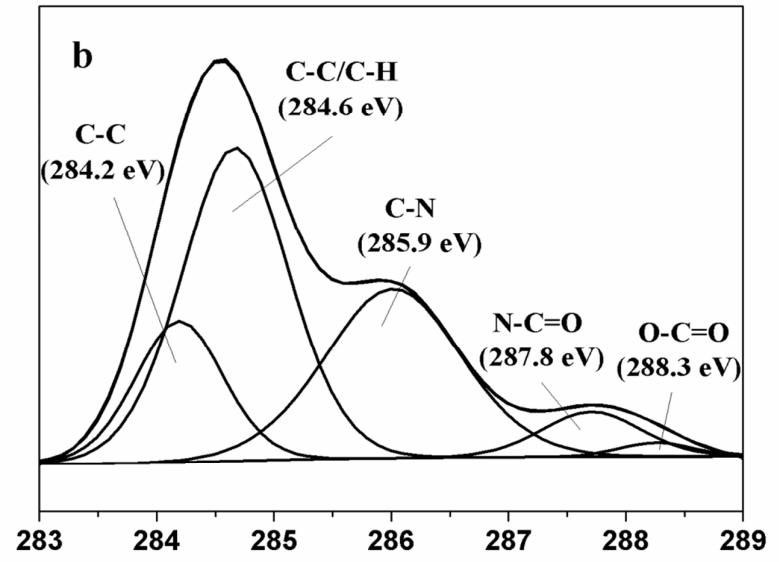

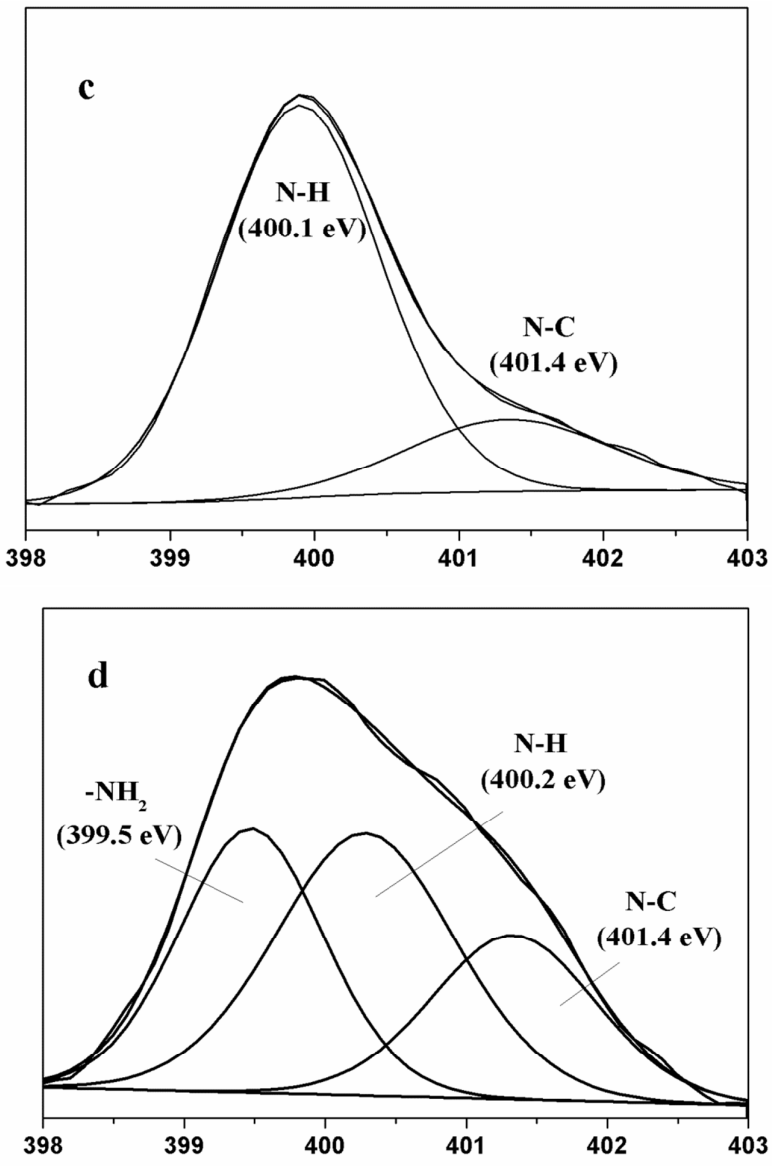

Fig. 3. -XPS spectra for the POD and the MPOD. a) C1s XPS spectrum of POD. b) C1s XPS spectrum of MPOD. c) N1s XPS spectrum of POD. d) N1s XPS spectrum of MPOD.

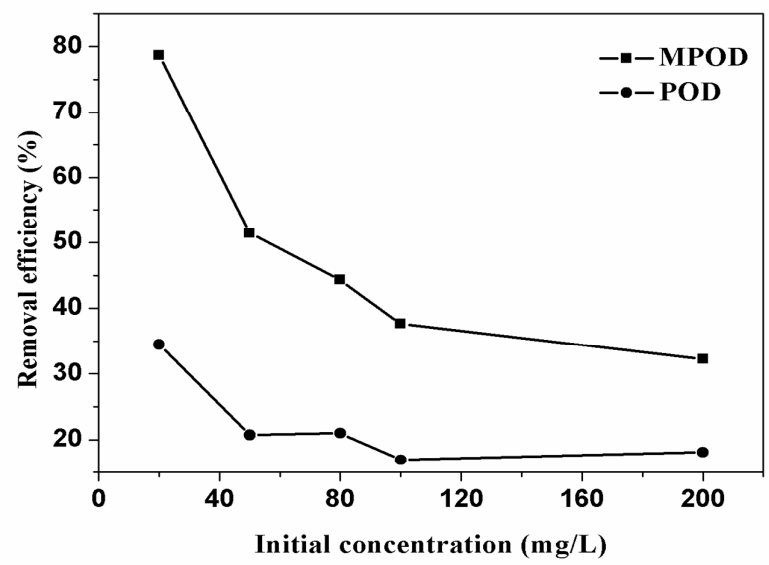

Fig. 4. Influence of initial concentration on Cr(VI) adsorption by POD and MPOD.

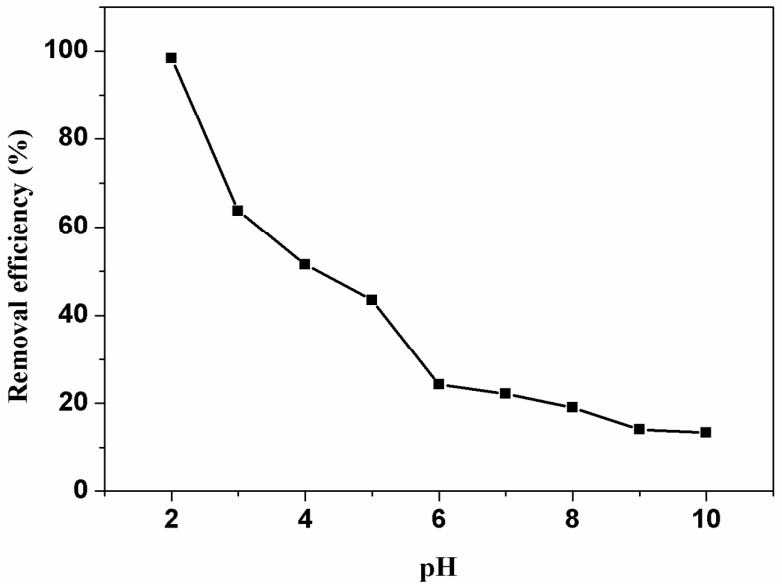

Fig. 5. Influence of solution pH on Cr(VI) adsorption by MPOD.

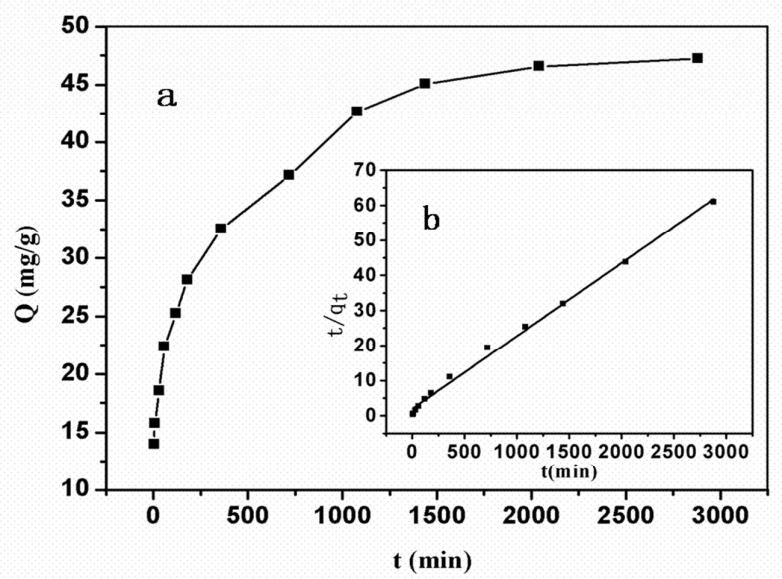

Fig.6. -Kinetics of Cr(VI) adsorption onto MPOD at 50 °C (initial Cr(VI) concentration 100 mg L^{-1}; pH: 2.0). a) Cr(VI) sorption kinetics data; b) pseudo second-order model for Cr(VI) sorption.

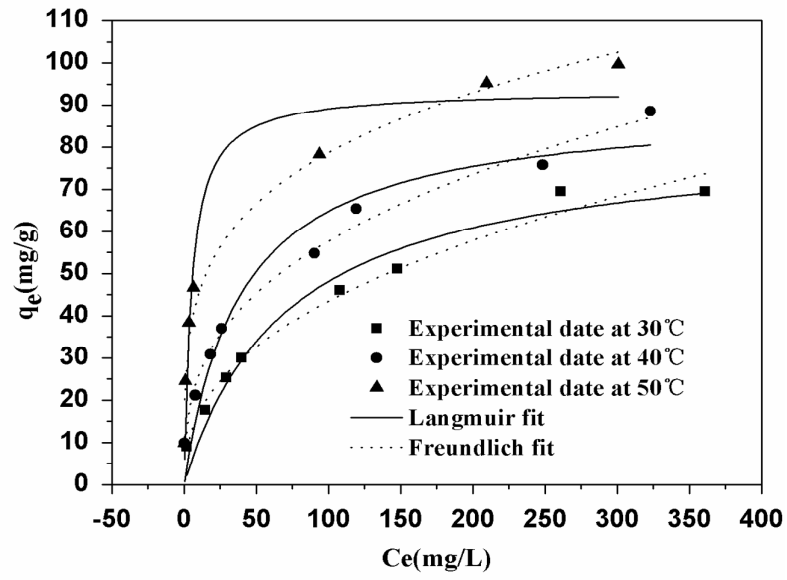

Fig.7. Langmuir and Freundlich isotherm for biosotption of Cr(VI) on MPOD (Cr(VI) solution volume: 50 mL; adsorbent dose: 0.1 g; contact time: 24 h; pH: 2.0).

Fig. 8.

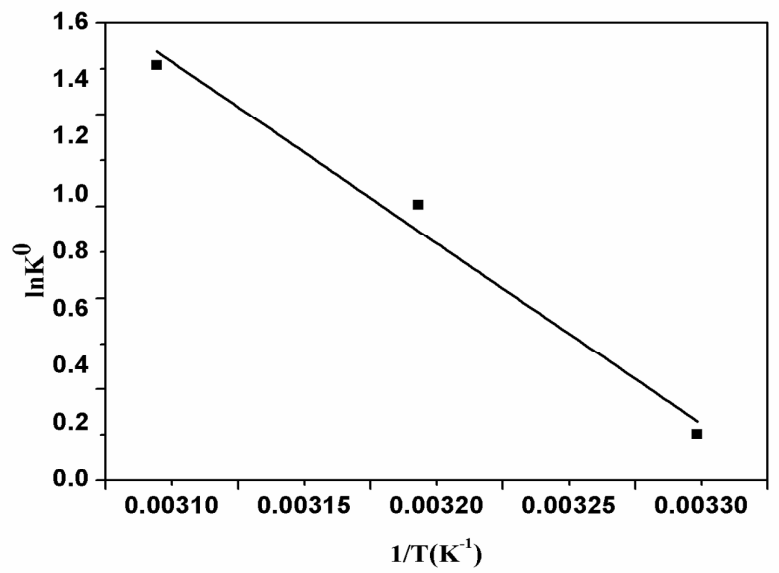

Fig. 8. Plot of lnK^0 versus 1/T for estimation of thermodynamic parameters for the biosorption of Cr(VI) on MPOD. (Volume, 50 mL; biosorbent dose: 2.0 g; initial Cr(VI) concentration: 20, 50, 80, 100, 200, 250, 400, 500 mg L^{-1}; pH: 2.0; contact time: 24 h.)

Tale 1 Kinetic parameters for biosorption of Cr(VI) on MPOD

C_0(mg L^{-1})	Pseudo-first-order			Pseudo-second-order		
	$q_{e,1}$ (mg g^{-1})	k_1 (min^{-1})	R^2	$q_{e,2}$ (g mg^{-1} min^{-1})	k_2 (min^{-1})	R^2
100	29.72	17.64	0.98	50	0.01	0.99

Table 2 Langmuir and Freundlich isotherm parameters for biosorption of Cr(VI) on MPOD

T(K)	Langmuir model			Freundlich model		
	q_m(mg g^{-1})	K_L(L mg^{-1})	R^2	K_f(L mg^{-1})	n	R^2
303.15	82.88	0.01	0.96	6.52	2.43	0.98
313.15	90.25	0.03	0.94	11.51	2.85	0.99
323.15	93.58	0.20	0.95	25.95	4.15	0.97

Table 3 Thermodynamic parameters for biosorption of Cr(VI) on MPOD

Temperature(K)	$\ln K^0$	ΔG^0(kJ mol^{-1})	ΔS^0(J K^{-1} mol^{-1})	ΔH^0(kJ mol^{-1})	R^2
303.15	0.16	-0.41	175.32	52.63	0.97
313.15	0.96	-2.51			
323.15	1.45	-3.90			